DOI: 10.32615/ps.2019.028 PHOTOSYNTHETICA 57 (1): 61-74, 2019

Photosystem photochemistry, prompt and delayed fluorescence, photosynthetic responses and electron flow in tobacco under drought and salt stress

K. KHATRI[*,**] and M.S. RATHORE[*,**,+]

Biotechnology and Phycology Division, CSIR-Central Salt and Marine Chemicals Research Institute (CSIR-CSMCRI), Council of Scientific and Industrial Research (CSIR), Bhavnagar (Gujarat- 364001), India[*]
Academy of Scientific and Innovative Research, CSIR, New Delhi, India[**]

Abstract

The present study aimed to understand the photosynthetic responses and chlorophyll fluorescence transient in tobacco under drought and salt stress. Net CO_2 assimilation rate, stomatal conductance, intercellular CO_2 concentration and transpiration rate decreased significantly under drought and salt stress. The maximum quantum efficiency of PSII and electron transport rate were lower in tobacco under drought and salt stress. The maximum carboxylation rate, maximum electron transport rate, triosephosphate utilization efficiency, and mesophyll conductance decreased under drought and salt stress, while dark respiration increased. A pool size of the electron acceptors on reducing side of PSII and activity of water-splitting complex on the donor side of the PSII decreased during drought and salt stress. Present results suggested upregulation of the photorespiratory pathway as a strategy to maintain the ribulose-1,5-bisphosphate regeneration for maintenance of photosynthesis under drought and salt stress. Chlorophyll fluorescence indicated the impaired electron transfer and changes in the architecture of light-harvesting complex in tobacco leaves under drought and salt stress.

Additional key words: multisignal fluorescence; nonphotochemical quenching; photochemistry; photosynthetic performance; photorespiration.

Introduction

Photosynthesis is one of the key processes for existence of life. Plants under *in vivo* conditions are exposed to different kinds of stresses, *e.g*., light, drought, salinity, temperature, *etc*. These stresses negatively affect the photosynthesis through imposing the oxidative stress. Plants modulate their biochemical composition and physiology in order to adapt to prevailing environmental conditions. The most common environmental stresses are salt and drought stress. Both are interrelated as the salt stress is a kind of physiological drought. The molecular pathways leading to plant's adaptation under these two stresses overlap in various aspects. Under saline and drought conditions, an increased solute potential minimizes the stress-induced toxicity and maintains water contents and ionic homeostasis for optimal physiology. Plants conserve water by increasing water absorption or decreasing water loss through stomata (Thomas and Gausling 2000). Under such situation, the stomatal conductance (g_s) must decrease thereby reducing the photosynthetic gas exchange. The stomatal closure further reduces the cooling procedure and this causes accumulation of heat. Under such conditions, with limited CO_2 assimilation, the water–water cycle cannot eliminate excess excitation energy by acting as a major alternative electron sink (Driever and Baker 2011). Further, under low CO_2 concentration, the Rubisco causes increased oxygenation of ribulose-1,5-bisphosphate (RuBP) and higher Rubisco contents accelerate the rate of oxygenation. On the other hand, available light energy continuously induces electron transport which might lead to photoinhibition. The RuBP oxygenation produces one molecule each of glycolate-2-phosphate and glycerate-3-phosphate. The glycerate-3-phosphate

Received 16 June 2017, *accepted* 20 July 2018.
[+]Corresponding author; e-mail: mangalrathore@csmcri.res.in, mangalrathore@gmail.com.
Abbreviations: Chl – chlorophyll; C_i – intercellular CO_2 concentration; Car – carotenoids; DAB – 3,3-diaminobenzidine; DM – dry mass; E – transpiration rate; ETR – electron transport rate; FM – fresh mass; g_m – mesophyll conductance; g_s – stomatal conductance; J_0 – oxygenation; J_C – electron flow through PSII to RuBP carboxylation; J_{max} – maximum electron transport rate/electron transport capacity; NBT – nitroblue tetrazolium; NPQ – nonphotochemical quenching; PEG – polyethylene glycol; Φ_{PSII} – efficiency of PSII; P_N – net CO_2 assimilation rate; P_N-C_i – CO_2-response curve; q_P – photochemical quenching; R_D – dark respiration; RH – relative humidity; RuBP – ribulose-1,5-bisphosphate; TM – turgid mass; TPU – triosephosphate utilization; V_{cmax} – maximum carboxylation rate; WUE – water-use efficiency.
Acknowledgment: Authors thankfully acknowledge the CSIR, Govt. of India for financial support (OLP0079). Ms. Khatri is thankful to Council of Scientific and Industrial Research, New Delhi for financial support in the form of Junior Research Fellow. CSIR-CSMCRI PRIS 078/2017.

enters into the Calvin cycle and glycolate-2-phosphate, which act as chloroplast inhibitor, has to be converted into glycerate-3-phosphate. It was hypothesized that under stress conditions, plants manage optimum photosynthesis through altering their photorespiration and accelerating the RuBP regeneration (Huang *et al*. 2014).

The physiological alterations along with morphological modifications allow plants to cope with a broad range of environmental stresses. Photosynthetic measurements are important to understand the physiological responses of plants under different stress conditions. Various environmental stresses are known to lower down the photosynthesis in plants. The simultaneous gas-exchange and fluorescence measurement are commonly used in plant stress analysis (Ashraf and Harris 2013). The simultaneous measurement of gas exchange and fluorescence indicate the net CO_2 assimilation rate (P_N), intercellular CO_2 concentration (C_i), mesophyll conductance (g_m), transpiration rate (E), efficiency of PSII (Φ_{PSII}), photochemical quenching (q_p) and nonphotochemical quenching (NPQ), electron transport, and PSII photochemistry. Further, the CO_2-response curve (P_N–C_i; the photosynthentic rate plotted against intercellular CO_2 concentration) and light-response curve (the photosynthetic rate plotted against light intensity) help figure out the maximum carboxylation rate, triosephosphate utilization, day respiration, mesophyll conductance, rate of photosynthetic electron transport supporting $NADP^+$ reduction for RuBP regeneration, electron flow through PSII to RuBP carboxylation and oxygenation (Huang *et al.* 2014). These parameters indicate the physiological health of the plant and are used to assess the tolerance or adaptation under stress conditions.

The applications of chlorophyll (Chl) fluorescence are widely used in plant stress analysis (Kalaji *et al*. 2014, 2016 Lazár 2015). The antenna Chl of PSII is a source of variable fluorescence and Chl *a* fluorescence measurement is being widely used for screening of stress tolerance in different plant species. The concepts and scientific insights related to Chl fluorescence measurements perceived new parameters for plant stress analysis. This resulted in development of new techniques and new commercial instruments (Salvatori *et al*. 2014) for simultaneous measurement of prompt (PF) and delayed fluorescence (DF) and modulated reflectance of P700 (Strasser *et al*. 2010, Kalaji *et al*. 2012). The PF is the fluorescence induction curve from minimum (F_0) to maximum (F_m) fluorescence in dark-adapted samples. The curve is known as fluorescence transient (FT) and represents the fast kinetics of fluorescence emission (Strasser *et al*. 2010); its normalized analysis is called JIP-test (Strasser *et al*. 2004). The OJIP transient reflects the kinetic properties of the electron transport chain and provides information on the redox states of PSII and efficiencies of electron transfer during photosynthetic electron transport chain. The DF occurs after PF decay, and it is a form of light emitted by plants mainly from PSII (Krasteva *et al*. 2013) in the red-infrared region once they are exposed to light. The DF occurs after electrons transfer backward in the photosynthetic chain and reflect the recombination between the reduced electron acceptor Q_A^- and the oxidized secondary electron donor Z^+ of PSII (Salvatori *et al*. 2014). Measurements of prompt and delayed Chl *a* fluorescence have been used to investigate photosynthesis under abiotic stress conditions, *i.e*., PSII electron donor side, electron transport between PSII and PSI, and PSI electron acceptor side (Strasser *et al*. 2010, Oukarroum *et al*. 2013, 2016; Gao *et al*. 2014). Protection of PSII and PSI photochemistry under drought stress through adjustment of the energy distribution between photosystems and activation of alternative electron sinks has been reported by Chl fluorescence measurement (Zivcak *et al*. 2013). Recent literature reports showed changes in PSII quality and functioning under different kinds of stresses (Kalaji *et al*. 2016). Drought stress inhibits reoxidation of Q_A^- and suppresses the quantum yields of photoinduced electron transport in PSII reaction center to Q_A (Goltsev *et al*. 2012). Salinity stress has been reported to cause more damage on the donor side of PSII as compared to the acceptor side (Mehta *et al*. 2010).

During exposure of plants to stress conditions, the early responses are of critical significance. The early responses of the photosynthetic apparatus in plants play an important role in their tolerance to salt stress (Kalaji *et al*. 2011). In this work, we used infrared gas analyzer (*LI-6400XT*; *Li-Cor*, Lincoln, NE, USA) and multifunctional plant efficiency analyzer (*MPEA-2*; *Hansatech Instruments*, UK) to understand the photosynthetic responses and Chl fluorescence transient in tobacco subjected to salt and drought stress for a short (24-h) duration. The aim of this study was to understand photosystem photochemistry, PF, DF, photosynthetic responses, light and P_N–C_i response curve, and electron flow through photosynthetic and photorespiratory pathway during photosynthesis in tobacco under drought and salt stress. The results would be useful to understand the photosynthetic performance of plants under stress conditions. Further, the results would establish a linkage between photorespiration and photosynthesis in plants under stress conditions. The results would add some knowledge to our understanding of photosynthetic responses in a model plant, *i.e.,* tobacco under salt and drought stress, which would serve as a base for functional validation of salt and drought-responsive genes. The results on a model plant could be easily used as a ready-made reference by the researcher for interpretation of results on functional validations of transgenic tobacco for the development of drought and salt tolerance.

Material and methods

Seed germination, plant growth, and stress treatments: The seeds of tobacco (*Nicotiana tobacum* L., cv. Petit Havana) were germinated and grown on ½ strength of hormone-free 0.7% agar-gelled Murashige and Skoog's (MS) basal medium (Murashige and Skoog 1962) for two weeks in a culture room under 12-h photoperiod at PPFD of 150 μmol(photon) m^{-2} s^{-1}, 25 ± 1ºC, and 60% relative humidity (RH). Two weeks-old seedlings were cultured hydroponically in the ½ strength of Hoagland salt (without any chloride salt solution). These were grown for six weeks in a growth chamber (*PGC-105*, *Percival Scientific*, USA)

at 25 ± 1ºC, 60% RH, ambient CO_2 concentration, and 12-h photoperiod with a light intensity of 1,000 µmol(photon) m^{-2} s^{-1}. The six weeks-old plants (n = 3) were subjected to drought [5 and 10% solution of polyethylene glycol-6000 (*PEG-6000*, *Hi-Media*, India)], and salt [0.1 and 0.2 M solution of sodium chloride (NaCl, *Hi-Media*, India)] stress individually for 24 h and the photosynthetic responses were recorded. After stress treatments, the samples were harvested, and physio-chemical analysis was carried out.

Determination of solute potential, relative water contents, and photosynthetic pigments: Leaf samples from control and stressed plants were frozen in liquid nitrogen, thawed, and centrifuged for 10 min at 10,000 × g to obtain the sap. Solute potential (Ψ) of the sap was measured by vapor pressure osmometer (*Wescor Inc*., Logan, UT, USA).

Leaf discs of approximately 200 mg fresh mass (FM) from control and treated plants were immersed in the deionized water for 18 h, and the turgid mass (TM) were recorded. Samples were dried at 80°C for 48 h in a hot air oven, and the dry mass (DM) was recorded. Relative water content (RWC, %) was calculated as (FM – DM)/(TM – DM) × 100.

Photosynthetic pigments were extracted in chilled N, N-dimethylformamide and the absorption was recorded at 461, 647, 664, and 664.5 nm using a UV-Visible spectrophotometer (*SpectramaxPlus 384*, *Molecular Devices*, USA). Chl contents were calculated following Inskeep and Bloom (1985), and the carotenoids (Car) were calculated following Chamovitz *et al*. (1993).

Light- and CO_2-response curve: Plants were exposed to PPFD of 1,200 µmol(photon) m^{-2} s^{-1} s and 380 µmol(CO_2) mol^{-1} for 45 min to obtain a steady state before generating light- and CO_2-response curves. The light-response curve was generated using an auto-program feature of the infrared gas analyzer (IRGA) system at an ambient CO_2 concentration [set at 380 µmol(CO_2) mol^{-1} using mixer facility of the instrument). The parameters of light-response curve were assessed stepwise at every 2 min at 2,500; 2,000; 1,600; 1,200; 800, 600, 400, 200, 100, 50, 20, and 0 µmol(photon) m^{-2} s^{-1}. CO_2-response curve was generated using an auto-program feature of the IRGA system at PPFD of 1,200 µmol(photon) m^{-2} s^{-1}. The parameters of CO_2-response curve were assessed stepwise at every 3 min at 400, 300, 200, 100, 50, 500, 600, 800; 1,000; 1,400; 1,800; 2,000; and 2,200 µmol mol^{-1}. The light and P_N–C_i response curves were fitted using curve fitting facilities (Sharkey *et al*. 2007, Sharkey 2016) and the maximum carboxylation rate (V_{cmax}), maximum electron transport rate (J_{max}) triosephosphate utilization (TPU), day respiration (R_D) mesophyll conductance (g_m) Rubisco content, electron flow through PSII to RuBP carboxylation (J_C) and oxygenation (J_0) were determined.

Gas exchange and pulse modulated Chl fluorescence were measured simultaneously using a leaf chamber fluorometer (*6400-40 LCF*, *Li-Cor*, USA) attached to an infrared gas analyzer (*LI-6400XT*; *Li-Cor*, Lincoln, NE, USA). Plants were dark-adapted for 45 min using dark facilities. The minimal fluorescence level (F_0) in the dark-adapted state was measured using a modulated pulse, while maximal fluorescence (F_m) was measured after applying a saturating actinic light. Steady-state fluorescence yield (F_s) and maximum fluorescence yield (F_m') were recorded using saturating actinic light pulse after adapting plants to PPFD of 1,200 µmol(photon) m^{-2} s^{-1} at 25 ± 1ºC and 60% RH for 45 min in a growth chamber. Measurements (three replicates per treatment and three readings per replicate, n = 9) were carried out on leaves acclimatized for 10 min to the leaf chamber conditions. Measurements were recorded at 1,200 µmol(photon) m^{-2} s^{-1}, 380 µmol(CO_2) mol^{-1}, 26 ± 1ºC block temperature, and 60 ± 5% RH. The P_N, C_i, g_s and E were recorded. Water-use efficiency (WUE) was calculated as P_N/E. Fluorescence parameters determined at light- and dark-adapted states, such as electron transport rate (ETR), maximum efficiency of PSII (F_v/F_m), the efficiency of PSII (Φ_{PSII}), photochemical (q_P), and nonphotochemical (NPQ) quenching, were used. The ETR through PSII was calculated as $J_T = [(F_m' - F_s)/F_m'] f I \alpha_{leaf}.$, where I is incident photon flux density [µmol(photon) m^{-2} s^{-1}], α_{leaf} is leaf absorbance typically assumed to be 0.85 and f is the fraction of absorbed quanta used by PSII. The f is typically assumed to be 0.5 based on the assumption of an equal distribution of photons between PSI and II (Miyake *et al*. 2005).

Multisignal Chl fluorescence was measured using multifunctional plant efficiency analyser (*MPEA-2*, *Hansatech*, UK). Measurements were recorded at room temperature on the adaxial surface of the fourth leaf from the top through continuous excitation with high-time resolution to investigate the rapid fluorescence induction (Oukarroum *et al.* 2015). The plants were dark-adapted for 45 min under ambient CO_2 at 25 ± 1°C using dark-adaptation facilities before the measurements of the Chl fluorescence. Leaves were illuminated with saturating red light of 3,000 µmol(photon) m^{-2} s^{-1} in order to close PSII reaction centers completely, and the fluorescence signals were recorded for 1.0 s on a 4-mm diameter area of a dark-adapted intact leaf. The PF and DF detector used 730 ± 15 nm wavelength of 3000 µmol(photon) m^{-2} s^{-1} intensity. The instrument recorded PF and DF when the actinic light was on (light interval) and off (dark interval), respectively. The recorded data were downloaded into *M-PEA Plus* software (*version 1.10*) and comprehensive analysis was performed with its data analysis module.

Different kinetic parameters calculated of Chl *a* fluorescence recording were summarized as Table 1S (*supplement*). In PF curve, $\delta F_{IP} = (F_P - F_I)$ is the ratio of PSII:PSI, where F_P is maximum fluorescence measured after approximately 200 ms of illumination and F_I the fluorescence step that occurred after approximately 30 ms, and it was calculated following Schansker *et al*. (2005). The δV_{IP} was calculated as $[\delta V_{IP} = (F_m - F_{30ms})/(F_m - F_0)]$, and indicated the electron transport around the PSI to reduce the final acceptors (*i.e*., ferredoxin and NADP) of the electron transport chain (Schansker *et al*. 2005). The DF induction curve was analyzed following Goltsev *et al*. (2009) and Oukarroum *et al*. (2013). Initial minimum

value of DF was taken as D_0. First maxima of the induction curve (I_1) represented the photochemical accumulation of light-emitting states of the PSII RC or delayed fluorescence precursors and nonphotochemical increase of the delayed fluorescence due to the electrical gradient formed by PSI when P700 is oxidized (Goltsev *et al*. 2009). The second maxima (I_2) in the range of I–P phase of PF curve represented prolonged reopening of PSII RCs by electron transfer from the reduced Q_B to PQ before the reduction of the PQ pool. The final maxima (I_4) appeared during the slight decrease of the PF intensity and oxidation of P700. I_4 represented the formation of the proton gradient (Evans and Crofts 1973, Goltsev *et al*. 2009) that increases the rate constant of radiative recombination in the PSII RCs. The minimum of the DF curve (D_2) indicated of the reducing activity of the PSII complex. The ratio of I_1/I_2 and I_4/D_2 were calculated; this represented electron flow in PSII (Goltsev *et al*. 2012) and transmembrane proton gradient (Goltsev *et al*. 2005), respectively.

Estimating the carboxylation, rate of photosynthetic electron flow and photorespiration: Using P_N–C_i curve, the maximum carboxylation rate (V_{cmax}) allowed by Rubisco, rate of photosynthetic electron transport supporting $NADP^+$ reduction for RuBP regeneration (J_{max}), triose phosphate utilization (TPU), dark respiration (R_D), and mesophyll conductance (g_m), at the measurement light intensity, were inferred by P_N–C_i curve fitting facilities according to Sharkey *et al*. (2007) and Sharkey (2016). The electron flow through PSII to RuBP carboxylation (J_C) and oxygenation (J_0) was allocated following Sharkey *et al*. (2007) and Sharkey (2016). J_0 was calculated as $2/3 \times [J_T - 4 \times (P_N + R_D)]$, and J_C as $1/3 \times [J_T + 8 \times (P_N + R_D)]$, where P_N is CO_2 assimilation and R_D represents the rate of mitochondrial respiration. R_D was taken from the linear region of the light-response curve between PPFDs of 0–100 μmol(photon) m^{-2} s^{-1} and inferred following Sharkey *et al*. (2007). The Rubisco content was inferred using equation y = 35.3x + 6.6 according to Yamori *et al*. (2010), where x is Rubisco content (μmol m^{-2}), and y is V_{cmax} [μmol(CO_2) m^{-2} s^{-1}].

Sugar and starch contents: For extraction of soluble sugar contents, the preweighed fresh samples were extracted with 80% ethanol. The residual pellet left after extraction of sugar was digested with 52% perchloric acid for starch estimation. The soluble sugar and starch contents were estimated following anthrone–sulphuric acid method using 0.2% anthrone reagent in chilled and concentrated H_2SO_4. Glucose was used as standard and the absorbance was measured at 630 nm. Obtained values were multiplied by a factor of 0.9 to convert the glucose value to starch. Sugar and starch contents were expressed as moles per fresh mass.

Histochemical detection of H_2O_2, O_2^- and starch: Hydrogen peroxide and O_2^- radical accumulation were detected *in vivo* in leaves of stressed and unstressed tobacco. The samples were immersed in nitroblue tetrazolium (NBT) solution (1 mg ml^{-1} in 10 mM phosphate buffer; pH 7.8) at room temperature for 2 h, thereafter exposed to high irradiance for 12 h until blue spots showing accumulation of O_2^- appeared. The presence of H_2O_2 was detected by immersing the leaf samples in 3,3-diaminobenzidine (DAB) solution (1 mg ml^{-1} in 10 mM phosphate buffer; pH 3.8) at room temperature for 6 h in the dark, thereafter exposing to the light until brown spots showing accumulation of H_2O_2 appeared. Before documentation, the samples were washed with ethanol to bleach out the Chl. Samples showing dark color or stain were considered to contain more amount of H_2O_2 and O_2^-.

Histochemical localization of starch was performed (Yang *et al*. 2014) in plants grown under different levels of stress. The leaf discs were immersed in boiling (100ºC) water for 1 min. Subsequently, the samples were immersed in boiling ethanol (95%) for 10 min for bleaching. The decolorized leaf discs were stained with iodine (I_2) and potassium iodide (KI) solution (1:2) for 1 min. The background color was removed by boiling the stained plants in ethanol (95%) for 15 s. The samples were washed with ethanol (95%) at RT and visualized using *Canon Eos 760D* camera.

Statistical analysis: The experiment was performed in triplicate with a minimum of three biological replicates. The data were subjected to one-way analysis of variance (*ANOVA*) for analysis of variance to determine the significance among mean values of control and treated plants. *ANOVA* was followed by *Duncan*'s multiple range test (DMRT) for comparison of means. The data was presented as mean ± SE and significant differences in mean values of control and stressed plants by the DMRT at 0.05% probability level were denoted by different lowercase letters.

Results

Salt and drought stress altered the plant physiology: The drought and salt stress caused a significant decrease in solute potential; it reached minimum (more negative value) in tobacco grown under 0.2 M NaCl stress (Fig. 1S*A*, *supplement*). The RWC in leaves decreased significantly under stress (Fig. 1S*B*, *supplement*) conditions. The stresses caused a decrease in contents of photosynthetic pigments; the decrease was higher in plants grown under NaCl stress than that of PEG stress (Fig. 1*A,B*).

The accumulation of total soluble sugars in tobacco leaves increased significantly under drought and salt stress (Fig. 1S*C*, *supplement*). The increase was the highest in tobacco grown under 10% PEG stress. Under NaCl stress, the increase in soluble sugars was comparatively lower than that in the plants under PEG stress. Beside accumulation of soluble sugar contents, the starch contents were found significantly lower in tobacco grown under stress as compared with control (Fig. 1S*D*, *supplement*). Further, the *in vivo* localization of starch showed a lower accumulation of starch in tobacco leaves under stress conditions (Fig. 2*A*). The *in vivo* localization of H_2O_2 through DAB staining and O_2^- through NBT staining (Fig. 2*B,C*) in leaf discs showed stress-caused accumulation of

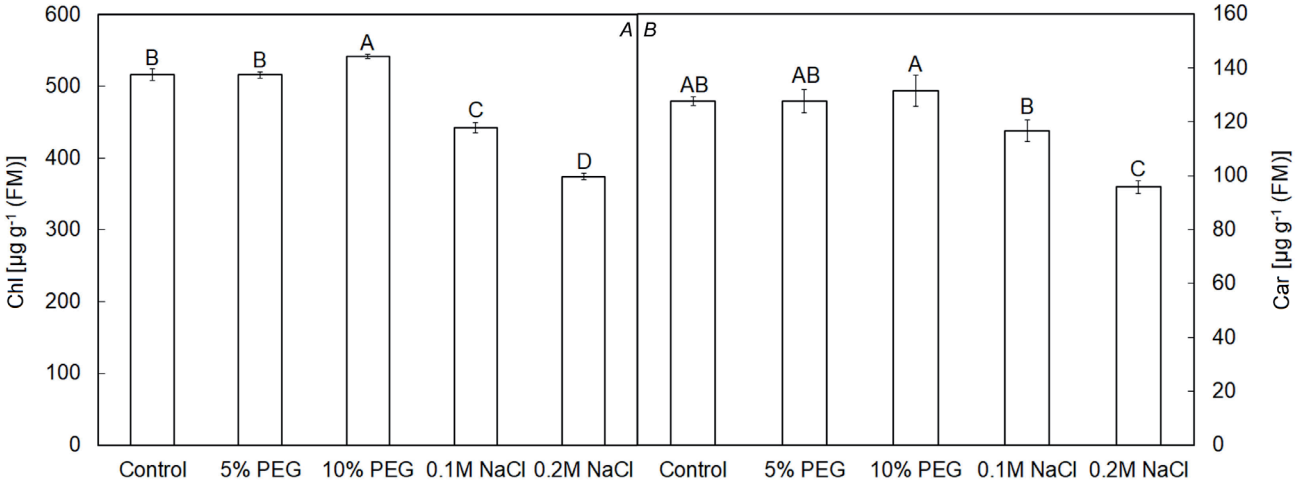

Fig. 1. Comparison of total chlorophyll (*A*), and carotenoids (*B*) contents in leaves of tobacco plants ($n = 3$) grown under control, 5% and 10% PEG, 0.1 M and 0.2 M NaCl stress.

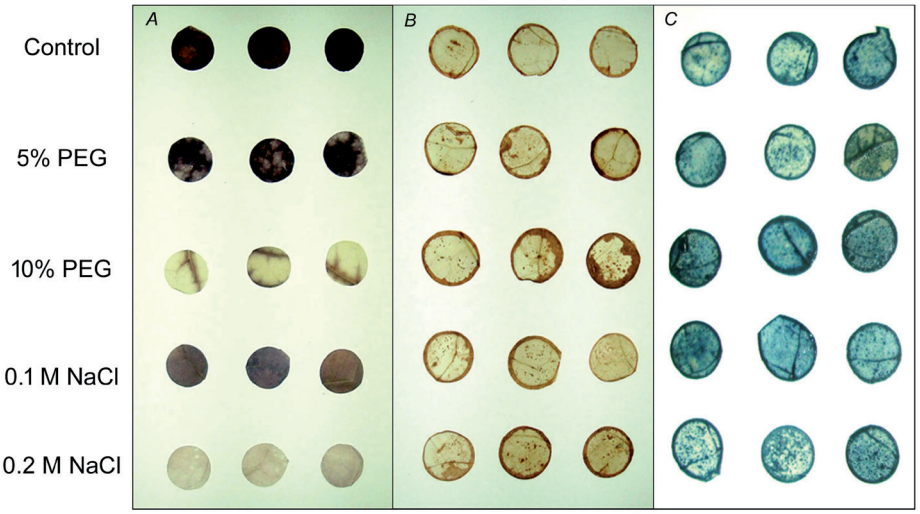

Fig. 2. *In vivo* localization and comparison of (*A*) starch, (*B*) H_2O_2, and (*C*) O_2^- in leaves of tabacco grown under control, 5% and 10% PEG, 0.1 M and 0.2 M NaCl stress.

reactive oxygen species (ROS) in leaves.

Stress reduced the gas exchange and photosynthetic performance: The P_N, g_s, C_i, and E decreased significantly under stress conditions (Fig. 3*A–D*). The decrease in photosynthetic measurements were found in accordance with the level of stress. The P_N and g_s were found strongly correlated ($r = 0.94$). Similarly, g_s had a direct influence on C_i ($r = 0.86$) and E ($r = 0.98$). The WUE varied accordingly and was estimated higher under stress conditions (Fig. 3*E*) because of stomatal closure and reduced transpiration.

The F_v/F_m was significantly lower in the plants under stress conditions as compared with control conditions. Φ_{PSII} was significantly lower in tobacco under stress conditions. Similarly, ETR was estimated significantly lower in tobacco under stress conditions as compared with control conditions. The P_N showed a positive correlation with Φ_{PSII} ($r = 0.97$) and ETR ($r = 0.97$). The NPQ increased under stress conditions. The q_P decreased significantly under stress conditions (Fig. 4*A–E*). The fluorescence parameters (F_v/F_m, Φ_{PSII}, ETR, NPQ, and q_P) showed a direct relation with P_N.

Stress influenced carboxylation, oxygenation, TPU, and electron flow through PSII and photorespiration: With an increase in PPFD, P_N increased in control and stress treatments, however, it was higher in control at given PPFD under stress conditions (Fig. 5*A*). Similarly, with an increase in CO_2 concentration and C_i, P_N increased in control and stress treatments. The P_N was higher in control at given Ci under stress conditions (Fig. 5*B*). The V_{cmax} decreased in tobacco under stress, and the decrease was more prominent under PEG stress as compared to NaCl stress. The J_{max} was estimated in accordance with V_{cmax} (Fig. 6*A,B*). The TPU decreased under stress conditions; this was more prominent under PEG stress. The R_D increased in tobacco leaves under stress conditions, and it was estimated the highest under NaCl stress. The g_m and Rubisco contents were lower under stress conditions (Fig. 6*B*). The J_C increased with light intensity and J_0 decreased with C_i under control, drought, and salinity stress conditions (Fig. 2S, *supplement*).

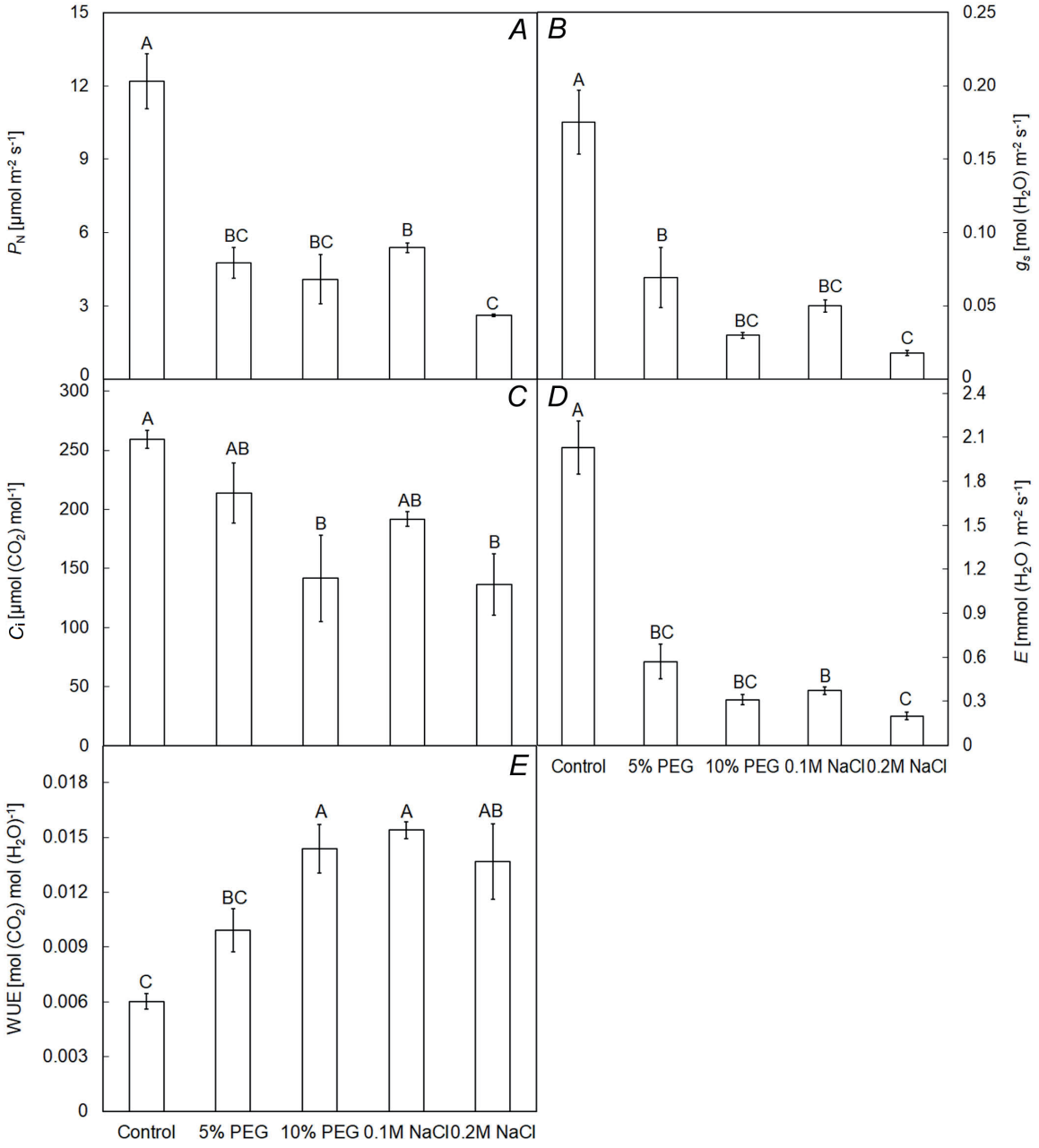

Fig. 3. Comparison of net CO_2 assimilation rate (P_N, *A*), stomatal conductance (g_s, *B*), intercellular CO_2 concentration (C_i, *C*), transpiration (*E*, *D*), and water-use efficiency (*E*) in leaves of tobacco (n = 9) grown under control, 5% and 10% PEG, 0.1 M and 0.2 M NaCl stress.

Multisignal fluorescence: From PF and DF measurements, various Chl fluorescence kinetic parameters were determined (Table 1S, *supplement*). The T_{Fm} is time to achieve F_m and it decreased in leaves of tobacco under stress conditions, however, it was significantly higher under 10% PEG stress. The area represents pool size of electron acceptors (Q_A) on reducing side of PSII and it was reduced significantly under stress conditions and was the lowest in leaves of tobacco under 10% PEG treatment. The emission by excited Chl *a* molecule in the PSII antenna (F_0) was higher under stress conditions and was found the highest in leaves of tobacco under 10% PEG stress. The maximum fluorescence (F_m) and the maximum capacity for photochemical quenching (F_v) were recorded lower in PEG treatments, while, after NaCl treatments, no statistically significant difference from the control was found. F_0/F_m increased under stress conditions, and it was significantly higher in leaves of tobacco under PEG stress. The maximum quantum efficiency of PSII (F_v/F_m) was lower under stress conditions. The F_V/F_0 was estimated lower under stress conditions. The V_J and V_I were estimated higher (Fig. 7*A*) under stress conditions. Both absorption (ABS/RC) and dissipation per reaction centre (DI_0/RC) were recorded higher under stress conditions. TR_0/RC in leaves of tobacco increased under stress conditions and the increase was higher under PEG stress. The ET_0/RC and

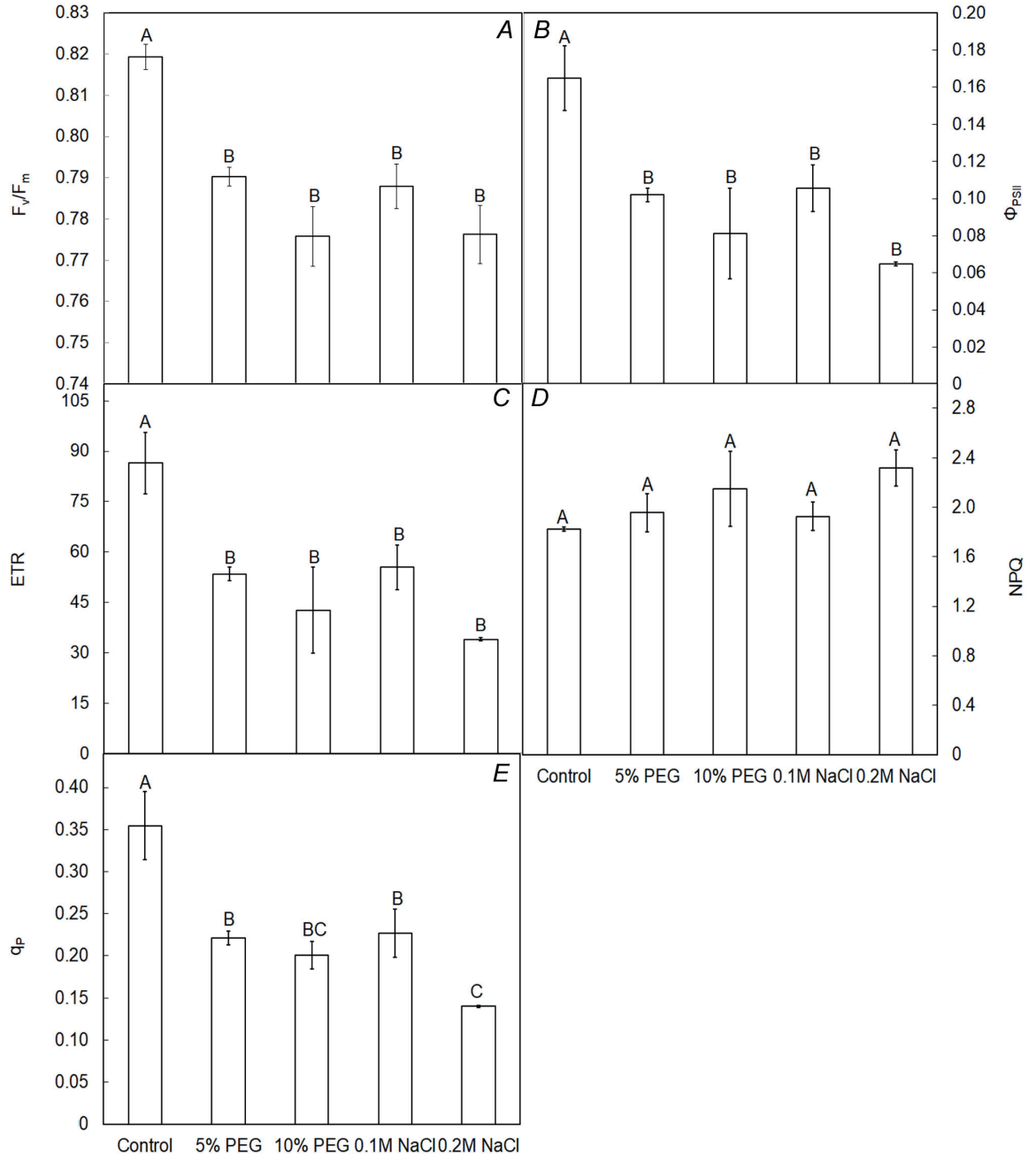

Fig. 4. Comparison of maximum quantum efficiency of PSII photochemistry (F_v/F_m, *A*), efficiency of PSII (ϕ_{PSII}, *B*), electron transport rate (ETR, *C*), nonphotochemical quenching (NPQ, *D*), and photochemical quenching (q_P, *E*) in leaves of tobacco ($n = 9$) grown under control, 5% and 10% PEG, 0.1 M and 0.2 M NaCl stress.

RE_0/RC were reduced significantly under stress conditions. ABS/CS_0, DI_0/CS_0, and TR_0/CS_0 increased in leaves of tobacco under PEG and the increase was insignificant under NaCl stress. The ABS/CS_0 is PSII activity in terms of cross-section, and it is in accordance with ABS/RC. ET_0/CS_0 and RE_0/CS_0 decreased with increasing stress (Fig. 7*B*). The $\gamma(RC)/[(1- \gamma(RC)]$, $\Phi(P_0)/[(1 - \Phi(P_0)]$ and $\psi(E_0)/[1 - \psi(E_0)]$ reflect portion of absorbed energy reaching RC, activity of the water-splitting complex, and light-independent thermal reaction, respectively, and these declined under stress conditions. The $[\delta R_0/(1 - \delta R_0)]$ indicate primary photochemistry and was estimated higher under mild stress and was reduced significantly with increased stress. The PI_{Total} was found lower under stress treatments. The driving force based on absorption basis (DF_{abs}) and energy conservation from absorbed photons by PSII to reduction of PSI end acceptors (DF_{Total}) and nonphotochemical de-excitation rate constant (kP/ABS × kF) were lower under stress treatments (Fig. 7*C*). The accumulation of closed RCs ($\delta Vg/dt_0$) and the excitation energy transfer between the RCs ($\delta V/dt_0$) were significantly higher in tobacco under stress conditions. The

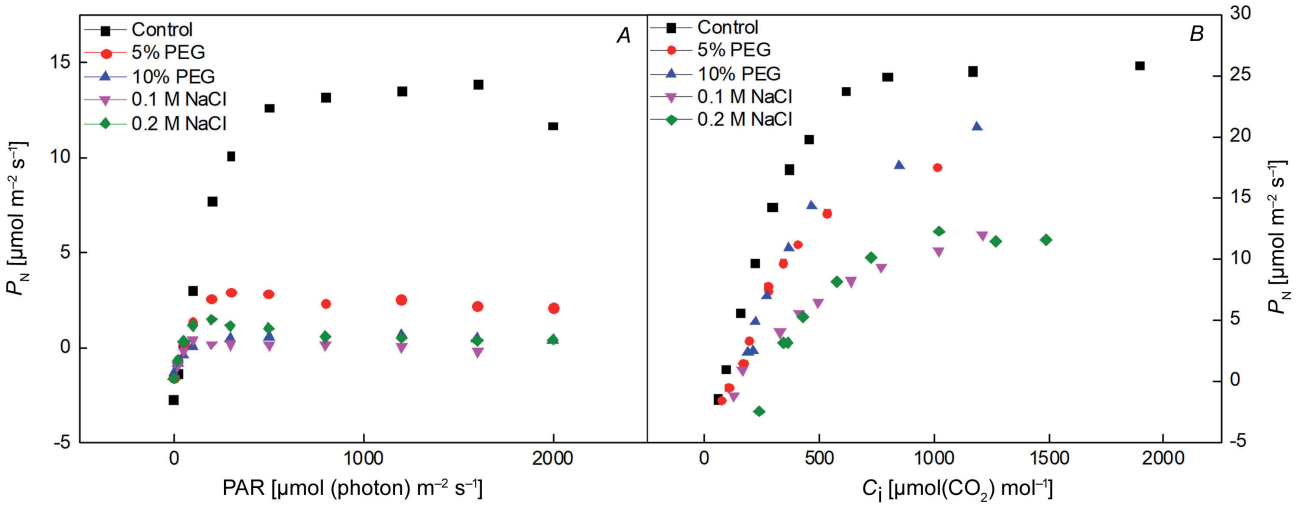

Fig. 5. Light- (*A*) and CO_2-response curve (P_N–C_i, *B*) in leaves of tobacco (n = 3) under control, 5% and 10% PEG, 0.1 M and 0.2 M NaCl stress.

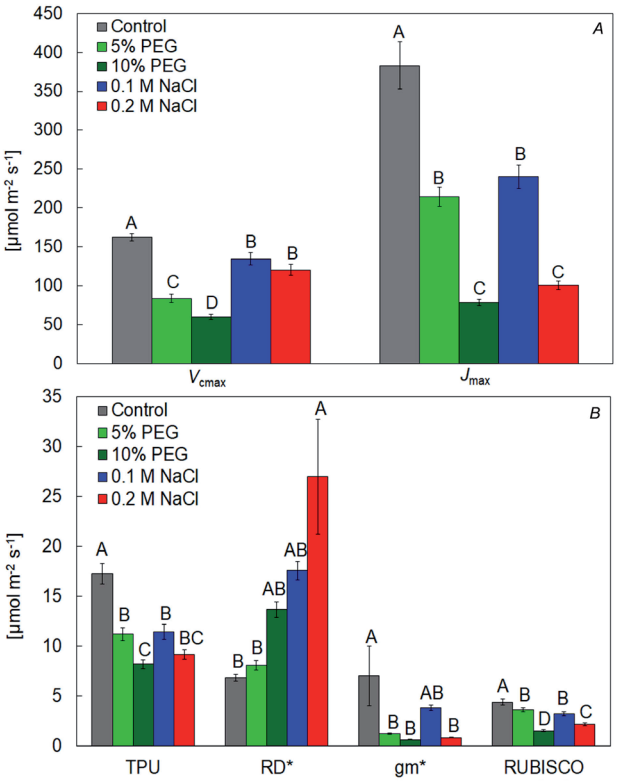

Fig. 6. Comparison of maximum carboxylation rate (V_{cmax}), maximum electron transport rate/electron transport capacity (J_{max}), triose phosphate utilization (TPU), dark respiration (R_D), mesophyll conductance (g_m), and Rubisco contents in leaves of tobacco plants (n = 3) grown under control, 5% and 10% PEG, 0.1 M and 0.2 M NaCl stress.

average redox state of Q_A (S_M/T_{Fm}) and maximum quantum yield of primary PSII photochemistry [$\Phi(P_0)$] were lower in tobacco under stress conditions. The efficiency of electron movement [$\psi(E_0)$] and quantum yield for electron transport [$\Phi(E_0)$] were significantly lower in stress treatments. The $\delta(R_0)$ (efficiency for an electron from the intersystem electron carriers to end electron acceptors at the PSI acceptor side) improved slightly under 5% PEG and 0.1 M NaCl, while decreased under higher stress. The $\Phi(R_0)$ (quantum yield for reduction of end electron acceptors at the PSI acceptor side) was reduced under stress conditions (Fig. 7*D*).

The kinetics of induction curve of PF and DF were plotted on a logarithmic time scale (Fig. 8*A,B*)**.** The PF curve showed O, J, I, and P phases. The DF showed a fast rise, polyphasic decline, and long-lasting plateau phase. The DF fast rises phase corresponded the rate of PF increase from J–I step and the polyphasic with I–P phase of the PF curve. The DF decreased under stress conditions and the values of δF_{IP} and δV_{IP} were reduced under stress conditions (Table 2S, *supplement*). The I_1/I_2 decreased in tobacco grown under 5% PEG and 0.1 M NaCl stress, thereafter increased. Similarly, the I_4/D_2 was reduced under stress conditions (Table 2S).

The ETR, estimated through modulated fluorescence measurement, was lower under stress conditions. Similarly in multisignal fluorescence measurements, the electron fluxes, such as ET_0/RC, RE_0/RC, ET_0/CS_0, and RE_0/CS_0, were lower in leaves of tobacco under stress conditions. The maximum quantum yields of primary PSII photochemistry [Φ_{PSII} and $\Phi(P_0)$] were found lower under stress conditions through both modulated and multisignal fluorescence. The Φ_{PSII} and CO_2 fixation (modulated fluorescence measurements) in tobacco leaves under stress conditions can be directly predicted by studying PI_{abs} and PI_{Total} (multisignal fluorescence measurements).

Discussion

The drought and salt stresses negatively affected the growth and development of tobacco plants and caused the significant decrease in solute potential, RWC, and photosynthetic pigments. The decrease in solute potential of sap, RWC in leaves and photosynthetic pigments have been reported under drought and salinity stress in

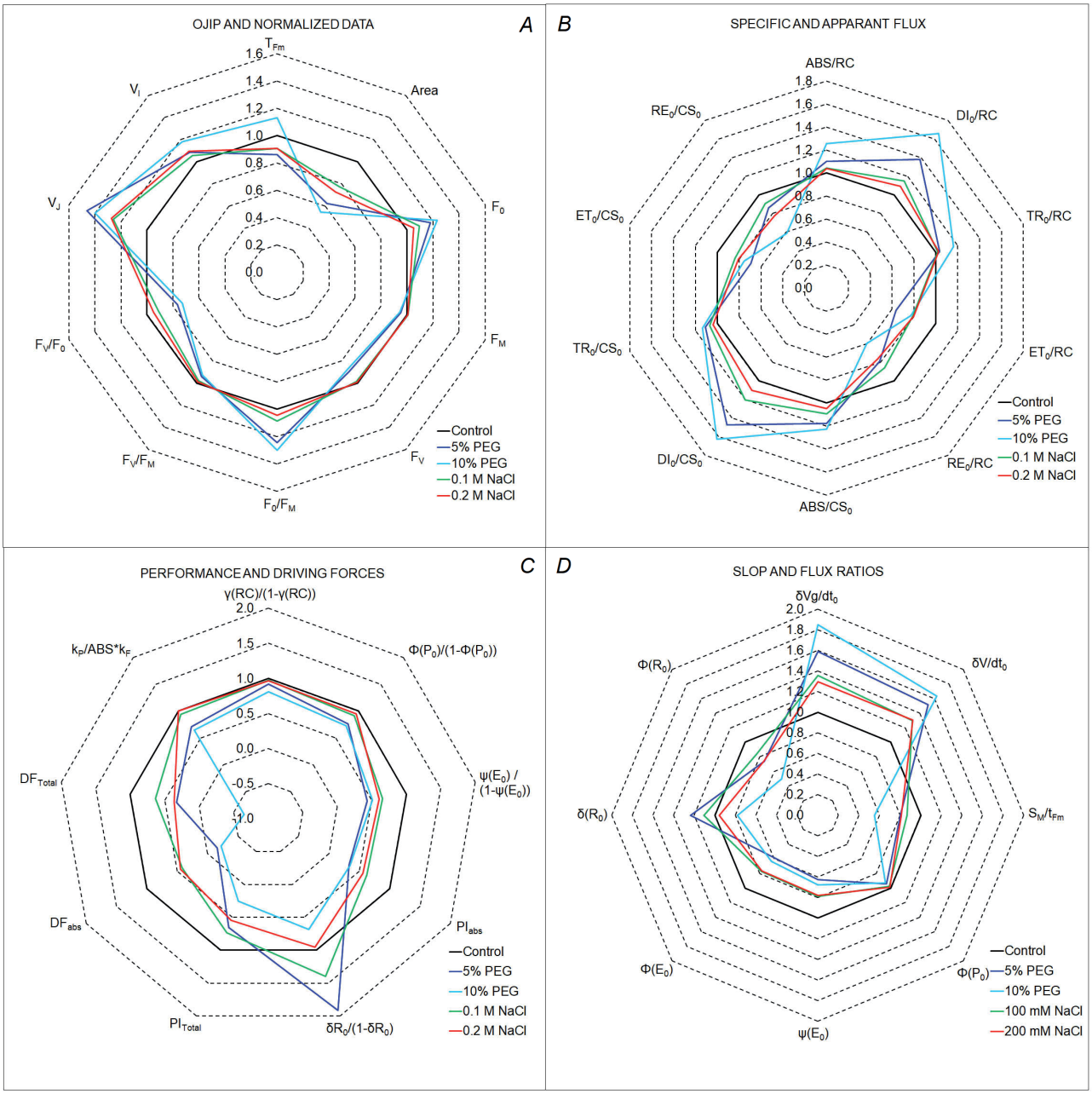

Fig. 7. Comparison of prompt and delayed fluorescence: The JIP and normalized data (*A*), specific and apparent fluxes (*B*), performance and driving forces (*C*) and slops and flux ratios (*D*) in leaves of tobacco plants (n = 9) under control, 5% and 10% PEG, 0.1 M and 0.2 M NaCl stress.

both glycophytes and halophytes (Haque *et al*. 2017). Maintenance of intracellular ion homeostasis is fundamental to physiology of plants. Lower solute potential under stress indicated plant's adaptation toward drought and salinity stress. Similar results were observed in different reports during functional validation of transgenes under drought and salt stress (Kumari *et al*. 2017). Under salinity stress, lower pigment contents have been attributed to reduced biosynthesis of Chl in sunflower leaves (Santos 2004). The reduction in photosynthetic pigments is important, and this has a direct relationship to stress tolerance (Ahmad *et al*. 2005) as the pigments represent plant's efficiency to harvest or dissipate the excess light energy in PSI and PSII. Stress-induced inhibition of pigment synthesis and plant's adaptive strategy to avoid photoinhibition by decreasing light capture (Choinski *et al*. 2003) might be reasons for lower contents of pigment. Under PEG stress, immediate withdrawal of water from leaves might have diluted the effect of stress and maintained the pigment concentration under short-term exposure.

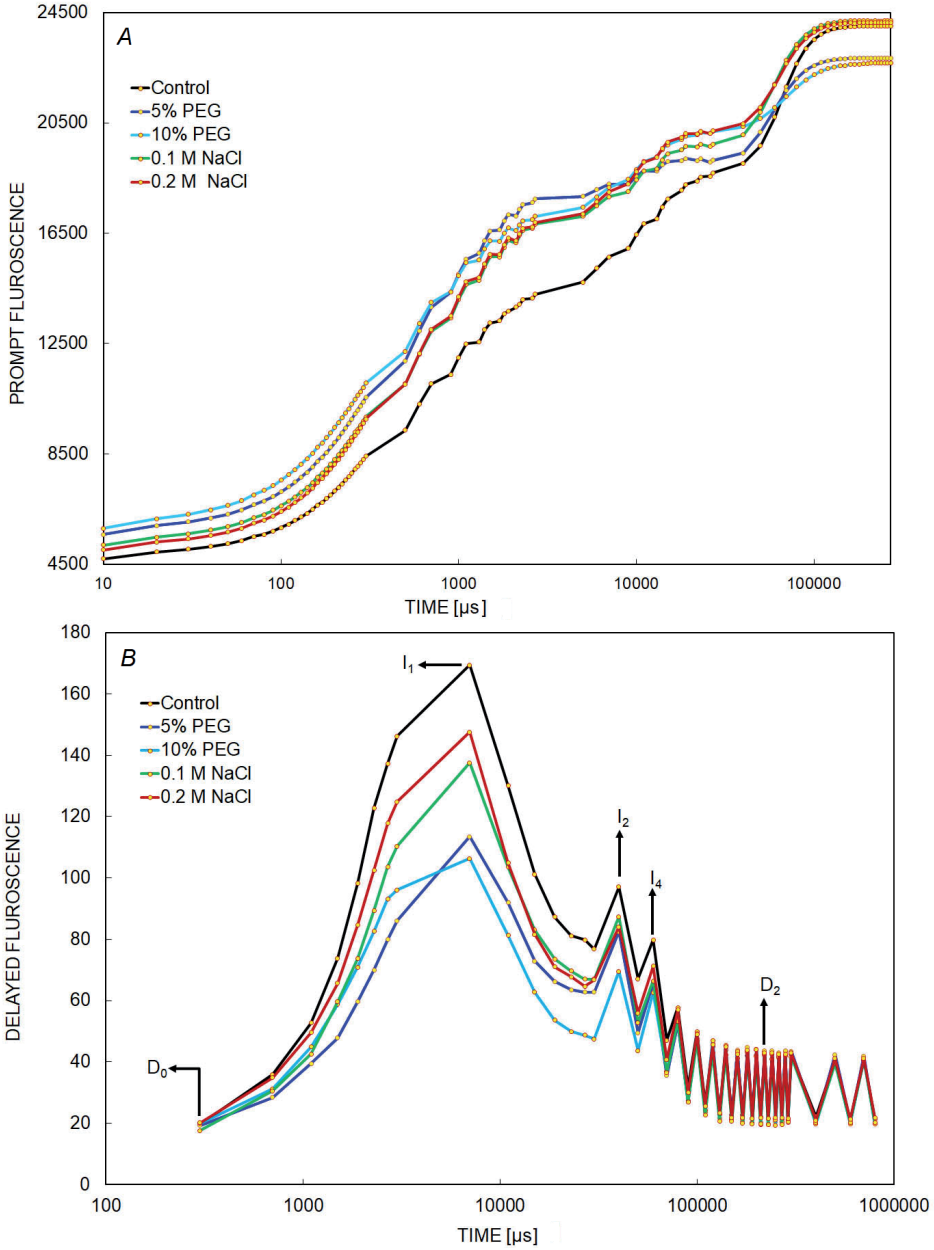

Fig. 8. The prompt (*A*) and delayed (*B*) fluorescence curves in leaves of tobacco plant grown under control and stress (drought and salt) conditions. The black, blue, pink, green, and red color represent the recording in the leaves of tobaccos (n = 9) under control, 5% and 10% PEG, 0.1 M and 0.2 M NaCl stress, respectively.

The accumulation of sugar, starch, and ROS varied under drought and salinity stress. Sucrose and starch synthesis have been reported to be tightly coupled with the rate of CO_2 assimilation (Foyer *et al.* 2000). A lower content of starch under stress conditions indicated accumulation of synthesized sugars as osmolytes and reduced conversion of synthesized sugar into starch. These results are in agreement with previous studies on different plant systems under stress conditions (Yang *et al*. 2014, Haque *et al*. 2017, Kumari *et al*. 2017). The *in vivo* localization of H_2O_2 and O_2^- clearly showed higher accumulation of ROS (Kumari *et al*. 2017), which might damage the metabolic machinery and thus affect photosynthesis negatively.

P_N is restricted by stomatal closure which limits diffusion of CO_2 and causes a decrease in C_i under stress conditions and ultimately results in a reduction of Rubisco activity (Maroco *et al.* 2002). In present study, the stress-induced changes in CO_2 assimilation could be accounted for changes in stomatal response. Under stress conditions, the stomatal limitation could be a reason for reduction in CO_2 assimilation and similar results were reported in previous studies (Flexas *et al.* 2004, Debez *et al*. 2008). The lower water content leads to stomatal closure; in our case, the lower RWC in tobacco leaves under stress conditions clearly indicated the stomatal closure. The higher WUE indicated the conservation of water under stress conditions probably due to the accumulation of organic solutes. Thus, the present results clearly indicated that stress caused alterations in g_s that was the primary factor controlling the P_N, C_i, E, and WUE. The lower g_s and E could be considered as an adaptive mechanism of plants as it helps reduce salt loading into leaves and maintain the

salt below a toxic concentration (Moradi and Ismail 2007). With lower CO_2 assimilation, the reduced activity of the Calvin-Benson (C_3) cycle under stress conditions could lead to an increased production of superoxide radicals on the acceptor side of PSI (Oukarroum *et al.* 2009).

The lower value of F_v/F_m showed the adverse effect of stress on light-utilization efficiency of tobacco plants under stress. The positive correlation of P_N with Φ_{PSII} and ETR showed a linear relationship among these parameters (Maxwell and Johnson 2000). The higher NPQ indicated dissipation of excess energy under stress conditions (Redondo-Gómez *et al*. 2006). The increase in NPQ is considered as a protective mechanism of the photosynthetic apparatus (Lawlor 2002). The decreased q_P under stress conditions (Netondo *et al*. 2004) indicated the lesser availability of energy for the photochemical purpose under stress conditions. The present results suggested that decreased rate of photosynthesis might occur due to direct effect of stress on stomatal conductance (Dionisio-Sese and Tobita 2000) and indirect effect of stress on photochemical functioning of plants (Moradi and Ismail 2007). The drought and salinity stress-induced limitation in P_N could lead to imbalance between PSII activity and electron requirements. This might result in over-excitation and photoinhibition thereof (Pérez-López *et al.* 2012).

The g_m was significantly lower in tobacco under stress conditions as compared to control (Flexas *et al.* 2004). Under stress conditions, decreased biosynthesis of Rubisco has been reported. Further, Rubisco activity in tobacco decreased due to accumulation of inhibitory molecules during stress. The J_C and J_0 indicated the electron flow devoted to the RuBP carboxylation and oxygenation, respectively (Fig. 2S). Differential activity of Rubisco has been reported in plants under stress conditions (Ashraf and Harris 2013). A significant reduction in Rubisco carboxylation activity, RuBP regeneration, and TPU utilization has been reported under stress conditions (Wilson *et al*. 2000, Maroco *et al*. 2002, Pérez-López *et al*. 2012). The decreased g_s caused decrease in g_m as the changes in g_m can be as rapid as changes in g_s (Centritto *et al*. 2003, Loreto *et al*. 2003). The stress affects diffusion of CO_2 in the leaves through a decreased g_s and g_m. This resulted in decreased CO_2 concertation in chloroplasts as compare to intercellular CO_2 concentration. The lower P_N in leaves of stress-affected tobacco was primarily due to decreased g_s and g_m. Further, the stress-induced degradation of large subunit of Rubisco (Lee *et al.* 2016) along with decreased g_s and g_m cause a reduction in biochemical capacity to assimilate CO_2 in tobacco leaves.

In multisignal fluorescence measurement, decreased T_{Fm} indicated stress conditions. Under 10% PEG stress, the relative increase in total Chl contents due to sudden withdrawal of water from leaf might be reason for increased T_{Fm}. The area represents pool size of electron acceptors (Q_A) on reducing side of PSII and the reduced area clearly indicated the blockage of electron transfer from reaction centers to quinone pool or at the donor side of PSII (Mehta *et al.* 2010). The increased F_0 in plants under stress conditions may be considered as an indicator of damage to PSII (Bussotti *et al.* 2011) and this indicates heat dissipation in an uncontrolled manner, producing an excess of excitation power within the leaf. The decrease in F_m may occur due to inhibition of electron transport at the donor side of the PSII causing accumulation of P_{680}^+ (Govindjee 1995) and decrease in the pool size of Q_A. The decreased F_m has been reported to be associated with an increase in nonphotochemical quenching. The increased F_0/F_m under stress conditions (Ranjbarfordoei *et al*. 2006) indicated nonphotochemical quenching. The F_v/F_m was reported lower under stress conditions (Netondo *et al*. 2004, Ranjbarfordoei *et al*. 2006, Salvatori *et al*. 2014) and this indicated reduction of the capacity of photosynthetic machinery for photochemical quenching of energy in PSII. The lower estimates of activity of water-splitting complex or oxygen evolving complex on the donor side of the PSII (F_v/F_0) under stress conditions (Ranjbarfordoei *et al*. 2006) is attributed to impairment in photosynthetic electron transport (Pereira *et al*. 2000). Similar to present study, Salvatori *et al*. (2014) observed higher V_J and V_I under stress conditions. The increased V_J under stress conditions revealed a loss of Q_A reoxidation capacity and inhibition of electron transport at the acceptor side of PSII. In canola, decrease in V_J was recorded during salt stress (Jafarinia and Shariati 2012). The higher absorption and dissipation under stress conditions were found in consonance with Kalaji *et al*. (2011), Mathur *et al*. (2013), and Demetriou *et al*. (2007). The higher F_0 indicated the increased antenna size with active and inactive reaction centers; the addition of inactive centers to antenna size might be cause for increased ABC/RC. Further Mathur *et al*. (2013) reported higher ABS/RC due to conversion of PSII units into heat sinks units along with inactive RCs. The inactive centers could not trap photons, leading to an increase in the amount of untrapped photons and thus to the increase of DI_0/RC (Mathur *et al*. 2013).

The increased TR_0/RC indicates inefficiency of re-oxidation of reduced Q_A^- or electron transfer to Q_B and this leads to a loss of energy as dissipation (Mathur *et al*. 2013). The ET_0/RC is maximum electron transport flux per PSII reaction center; it reflects the activity of the active reaction centers (Misra *et al*. 2001). In the present case, the reduced ET_0/RC indicates reduced rate of reopening of RCs through reoxidation of Q_A^-. Under saline conditions, both increase and decrease in ET_0/RC has been reported (Mathur *et al*. 2013, Demetriou *et al*. 2007). The Chl contents also influence ABS/RC and ABS/CS_0 (Misra *et al*. 2001). Stress-caused inactivation of reaction center may be the reason for lower ET_0/CS_0 (Mehta *et al*. 2010). Variations in ABC/CS_0 and DI_0/RC under stress conditions indicate changes in the architecture of light-harvesting complex (Fusaro *et al*. 2016). The reduced $\gamma(RC)/[(1 - \gamma(RC)]$ under stress conditions indicated low density of PSII reaction centers in PSII Chl antenna bed (Krüger *et al*. 2014). Further lower estimates of $\Phi(P_0)/[(1 - \Phi(P_0)]$ and $\psi(E_0)/[1 - \psi(E_0)]$ indicated reduced contribution of light reactions for primary photochemistry and of the dark reactions from Q_A^- to PC, respectively. The $[\delta R_0/(1 - \delta R_0)]$ estimates indicated higher contribution of PSI reducing its end acceptors under mild stress, which was reduced significantly under 10% PEG and 0.2 M NaCl

stress. Similar to present study, the performance index was reported lower under stress treatments (Oukarroum *et al*. 2015, Dąbrowski *et al*. 2016, Kan *et al*. 2017). The lower estimates of $\Phi(P_0)$ indicated the reduced efficiency of PSII. The lower estimates of $\Phi(R_0)$ showed reduced quantum yield for reduction of the end electron acceptors at the PSI acceptor side.

In the present study, plateau and decline in PF and DF appeared almost at the same time (Strasser *et al*. 2010). The I–P phase depends on electrons originating in PSII flowing through PSI and the transient block on the acceptor side of PSI (Schansker *et al.* 2005). The lower increase in I–P phase under stress conditions indicated reduced activity of PSI. The δF_{IP} and δV_{IP} are amplitudes of fluorescence and indicate the relative contribution of the I-to-P rise to the OJIP-rise (Oukarroum *et al*. 2015, Salvatori *et al*. 2015). These are also considered as semi-quantitative indicators for changes in the PSI content of a leaf. The DF has been reported to decrease under stress conditions (Zhang and Xing 2008). I_1/I_2 is inversely related to electron flow in PSII and was reported to be sensitive to mild stress (Goltsev *et al.* 2012). The I_1/I_2 indicated the improved electron flow in PSII in tobacco grown under 5% PEG and 0.1 M NaCl stress. The I_4/D_2, an indicator of transmembrane proton gradient (Goltsev *et al.* 2005, Salvatori *et al.* 2014), showed reduced proton gradient under stressed conditions. The present results clearly indicated the reduced biophysical performance of the photosynthetic system in tobacco under stress.

In the present study, the results obtained with gas exchange, modulated fluorescence, and multisignal fluorescence measurements were found co-related with each other. The reduced ETR and electron fluxes under stress conditions indicated impairment in electron transfer which ultimately resulted in lower Φ_{PSII}, CO_2 fixation, and performance indexes in tobacco. In consonance with these results, van Heerden *et al*. (2007) reported a good correlation of declining CO_2 assimilation capacity with declining PI_{abs}.

Conclusion: Drought and salt stress significantly influenced photosynthesis and PSII efficiency in tobacco plants. Drought and salt stress caused reduction in maximum carboxylation rate, RuBP regeneration, triose-phosphate utilization, and mesophyll conductance along with an increase in heat dissipation and day respiration. The increased day respiration supported the supply RuBP for photosynthetic fixation of CO_2 under stress conditions. Stress caused a reduction in the size of plastoquinone pool, the activity of the water-splitting complex, and performance index. Stress-induced variations in energy absorption, trapping, and dissipation per reaction center indicated the changes in the architecture of light-harvesting complex. The decreased stomatal conductance, dissipation of trapped energy as heat, impaired electron transfer at the donor side of the PSII causing accumulation of P_{680}^+, and changes in the architecture of light-harvesting complex were the principle reasons for the decreased photosynthetic performance under stress conditions.

References

Ahmad S., Wahid A., Rasul E.: Comparative morphological and physiological responses of green gram genotypes to salinity applied at different growth stages. – Bot. Bull. Acad. Sin. **46**: 135-142, 2005.

Ashraf M., Harris P.J.C.: Photosynthesis under stressful environments: an overview. – Photosynthetica **51**: 163-190, 2013.

Bussotti F., Desotgiu R., Cascio C. *et al*.: Ozone stress in woody plants assessed with chlorophyll *a* fluorescence. A critical reassessment of existing data. – Environ. Exp. Bot. **73**: 19-30, 2011.

Centritto M., Loreto F., Chartzoulakis K.: The use of low [CO_2] to estimate diffusional and non-diffusional limitations of photosynthetic capacity of salt- stressed olive saplings. – Plant Cell Environ. **26**: 585-594, 2003.

Chamovitz D., Sandmann G., Hirschberg J.: Molecular and biochemical characterization of herbicide-resistant mutants of cyanobacteria reveals that phytoene desaturation is a rate-limiting step in carotenoid biosynthesis. – J. Biol. Chem. **268**: 17348-17353, 1993.

Choinski Jr J.S., Ralph P., Eamus D.: Changes in photosynthesis during leaf expansion in *Corymbia gummifera* – Aust. J. Bot. **51**: 111-118, 2003.

Dąbrowski P., Baczewska A.H., Pawluśkiewicz B. *et al*.: Prompt chlorophyll *a* fluorescence as a rapid tool for diagnostic changes in PSII structure inhibited by salt stress in Perennial ryegrass. – J. Photoch. Photobio. B **157**: 22-31, 2016.

Debez A., Koyro H.W., Grignon C. *et al*.: Relationship between the photosynthetic activity and the performance of *Cakile maritima* after long-term salt treatment. – Physiol. Plantarum **133**: 373-385, 2008.

Demetriou G., Neonaki C., Navakoudis E. *et al*.: Salt stress impact on the molecular structure and function of the photosynthetic apparatus—the protective role of polyamines. – BBA-Bioenergetics **1767**: 272-280, 2007.

Dionisio-Sese M.L., Tobita S.: Effects of salinity on sodium content and photosynthetic responses of rice seedlings differing in salt tolerance. – J. Plant Physiol. **157**: 54-58, 2000.

Driever S.M., Baker N.R.: The water–water cycle in leaves is not a major alternative electron sink for dissipation of excess excitation energy when CO_2 assimilation is restricted. – Plant Cell Environ. **34**: 837-846, 2011.

Evans E.H., Crofts, A.R.: The relationship between delayed fluorescence and the H^+ gradient in chloroplasts. – BBA-Bioenergetics **292**: 130-139, 1973.

Flexas J., Bota J., Loreto F. *et al*.: Diffusive and metabolic limitations to photosynthesis under drought and salinity in C_3 plants. – Plant Biol. **6**: 269-279, 2004.

Foyer C.H., Ferrario-Méry S., Huber S.C.: Regulation of carbon fluxes in the cytosol: coordination of sucrose synthesis, nitrate reduction and organic acid and amino acid biosynthesis. – In: Leegood R.C., Sharkey T.D., von Caemmerer S. (ed.): Photosynthesis. Advences in Photosynthesis and Respiration. Pp. 177-203. Springer, Dordrecht 2000.

Fusaro L., Gerosa G., Salvatori E. *et al*.: Early and late adjustments of the photosynthetic traits and stomatal density in *Quercus ilex* L. grown in an ozone-enriched environment. – Plant Biol. **18**: 13-21, 2016.

Gao J., Li P.M., Ma F.W., *et al*.: Photosynthetic performance during leaf expansion in *Malus micromalus* probed by chlorophyll *a* fluorescence and modulated 820 nm reflection. – J. Photoch. Photobio. B **137**: 144–150, 2014.

Goltsev V., Chernev P., Zaharieva I. *et al*.: Kinetics of delayed chlorophyll *a* fluorescence registered in milliseconds time

range. – Photosynth. Res. **84**: 209-215, 2005.
Goltsev V., Zaharieva I., Chernev P. *et al*.: Delayed fluorescence in photosynthesis. – Photosynth. Res. **101**: 217-232, 2009.
Goltsev V., Zaharieva I., Chernev P. *et al*.: Drought-induced modifications of photosynthetic electron transport in intact leaves: analysis and use of neural networks as a tool for a rapid non-invasive estimation. – BBA-Bioenergetics **1817**: 1490-1498, 2012.
Govindjee: Sixty-three years since kautsky: chlorophylla fluorescence. – Aust. J. Plant Physiol. **22**: 131-160, 1995.
Haque Md. I., Rathore Mangal S., Gupta H. *et al*.: Inorganic solutes contribute more than organic solutes to the osmotic adjustment in *Salicornia brachiata* (Roxb.) under natural saline conditions. – Aquat. Bot. **142**: 78-86, 2017.
Huang W., Zhang S.B., Hu H.: Sun leaves up-regulate the photorespiratory pathway to maintain a high rate of CO_2 assimilation in tobacco. – Front. Plant Sci. **5**: 688, 2014.
Inskeep W.P., Bloom P.R.: Extinction coefficients of chlorophyll *a* and *b* in N,N-dimethylformamide and 80% acetone. – Plant Physiol. **77**: 483-485, 1985.
Jafarinia M., Shariati M.: Effects of salt stress on photosystem II of canola plant (*Brassica napus*, L.) probing by chlorophyll *a* fluorescence measurements. – Iran. J. Sci. Technol. **36**: 71, 2012.
Kalaji H.M., Govindjee, Bosa K. *et al*.: Effects of salt stress on photosystem II efficiency and CO_2 assimilation of two Syrian barley landraces. – Environ. Exp. Bot. **73**: 64-72, 2011.
Kalaji H.M., Goltsev V., Bosa K. *et al*.: Experimental *in vivo* measurements of light emission in plants: a perspective dedicated to David Walker. – Photosynth. Res. **114**: 69-96, 2012.
Kalaji H.M., Jajoo A., Oukarroum A. *et al*.: Chlorophyll *a* fluorescence as a tool to monitor physiological status of plants under abiotic stress conditions. – Acta Physiol. Plant. **38**: 102, 2016.
Kalaji H.M., Schansker G., Ladle R.J. *et al*.: Frequently asked questions about *in vivo* chlorophyll fluorescence: practical issues. – Photosynth. Res. **122**: 121-158, 2014.
Kan X., Ren J.J., Chen T.T. *et al*.: Effects of salinity on photosynthesis in maize probed by prompt fluorescence, delayed fluorescence and P700 signals. – Environ. Exp. Bot. **140**: 56-64, 2017.
Krasteva V., Alexandrov V., Chepisheva M. *et al*.: Drought induced damages of photosynthesis in bean and plantain plants analyzed *in vivo* by chlorophyll *a* fluorescence. – Bulg. J. Plant Physiol. **19**: 39-44, 2013.
Krüger G.H.J., De Villiers M.F., Strauss A.J. *et al*.: Inhibition of photosystem II activities in soybean (*Glycine max*) genotypes differing in chilling sensitivity. – S. Afr. J. Bot. **95**: 85-96, 2014.
Kumari J., Udawat P., Dubey A.K. *et al*.: Overexpression of SbSI-1, a nuclear protein from *Salicornia brachiata* confers drought and salt stress tolerance in tobacco by curtailing oxidative damage and maintaining photosynthetic efficiency. – Front. Plant Sci. **8**: 1215, 2017.
Lawlor D.W.: Limitation to photosynthesis in water-stressed leaves: stomata *vs*. metabolism and the role of ATP. – Ann. Bot.-London **89**: 871-885, 2002.
Lazár D.: Parameters of photosynthetic energy partitioning. – J. Plant Physiol. **175**: 131-147, 2015.
Lee B.R., Zaman R., Avice J.C. *et al*.: Sulfur use efficiency is a significant determinant of drought stress tolerance in relation to photosynthetic activity in *Brassica napus* cultivars. – Front. Plant Sci. **7**: 459, 2016.
Loreto F., Centritto M., Chartzoulakis K.: Photosynthetic limitations in olive cultivars with different sensitivity to salt stress. – Plant Cell Environ. **26**: 595-601, 2003.
Maroco J.P., Rodrigues M.L., Lopes C. *et al*.: Limitations to leaf photosynthesis in field-grown grapevine under drought-metabolic and modelling approaches. – Funct. Plant Biol. **29**: 451-459, 2002.
Mathur S., Mehta P., Jajoo A.: Effects of dual stress (high salt and high temperature) on the photochemical efficiency of wheat leaves (*Triticum aestivum*). – Physiol. Mol. Biol. Plant. **19**: 179-188, 2013.
Maxwell K., Johnson G.N.: Chlorophyll fluorescence – a practical guide. – J. Exp. Bot. **51**: 659-668, 2000.
Mehta P., Jajoo A., Mathur S. *et al*.: Chlorophyll a fluorescence study revealing effects of high salt stress on photosystem II in wheat leaves. – Plant Physiol. Bioch. **48**: 16-20, 2010.
Misra A.N., Srivastava A., Strasser R.J.: Utilization of fast chlorophyll a fluorescence technique in assessing the salt/ion sensitivity of mung bean and *Brassica* seedlings. – J. Plant Physiol. **158**: 1173-1181, 2001.
Miyake C., Horiguchi S., Makino A. *et al*.: Effects of light intensity on cyclic electron flow around PSI and its relationship to non-photochemical quenching of Chl fluorescence in tobacco leaves. – Plant Cell Physiol. **46**: 1819-1830, 2005.
Moradi F., Ismail A.M.: Responses of photosynthesis, chlorophyll fluorescence and ROS-scavenging systems to salt stress during seedling and reproductive stages in rice. – Ann. Bot.-London **99**: 1161-1173, 2007.
Murashige T., Skoog F.: A revised medium for rapid growth and bio assays with tobacco tissue cultures. – Physiol. Plantarum **15**: 473-497, 1962.
Netondo G.W., Onyango J.C., Beck E.: Sorghum and salinity. – Crop Sci. **44**: 797-805, 2004.
Oukarroum A., Bussotti F., Goltsev V., Kalaji H.M.: Correlation between reactive oxygen species production and photochemistry of photosystems I and II in *Lemna gibba* L. plants under salt stress. – Environ. Exp. Bot. **109**: 80-88, 2015.
Oukarroum A., El Madidi S., Strasser R.J.: Differential heat sensitivity index in barley cultivars (*Hordeum vulgare L.)* monitored by chlorophyll *a* fluorescence OKJIP. – Plant Physiol. Bioch. **105**: 102-108, 2016.
Oukarroum A., Goltsev V., Strasser R.J.: Temperature effects on pea plants probed by simultaneous measurements of the kinetics of prompt fluorescence, delayed fluorescence and modulated 820 nm reflection. – PLoS ONE **8**: e59433, 2013.
Oukarroum A., Schansker G., Strasser R.J.: Drought stress effects on photosystem I content and photosystem II thermotolerance analyzed using Chl *a* fluorescence kinetics in barley varieties differing in their drought tolerance. – Physiol. Plantarum **137**: 188-199, 2009.
Pereira W.E., de Siqueira D.L., Martínez C.A. *et al*.: Gas exchange and chlorophyll fluorescence in four citrus rootstocks under aluminium stress. – J. Plant Physiol. **157**: 513-520, 2000.
Pérez-López U., Robredo A., Lacuesta M. *et al*.: Elevated CO_2 reduces stomatal and metabolic limitations on photosynthesis caused by salinity in *Hordeum vulgare*. – Photosynth. Res. **111**: 269-283, 2012.
Ranjbarfordoei A., Samson R., Van Damme P.: Chlorophyll fluorescence performance of swee*t al*mond [*Prunus dulcis* (Miller) D. Webb] in response to salinity stress induced by NaCl. – Photosynthetica **44**: 513-522, 2006.
Redondo-Gómez S., Wharmby C., Castillo J.M. *et al*.: Growth and photosynthetic responses to salinity in an extreme halophyte, *Sarcocornia fruticosa*. – Physiol. Plantarum **128**: 116-124, 2006.
Salvatori E., Fusaro L., Gottardini E. *et al*.: Plant stress analysis: Application of prompt, delayed chlorophyll fluorescence and 820 nm modulated reflectance. Insights from independent

experiments. – Plant Physiol. Bioch. **85**: 105-113, 2014.
Salvatori E., Fusaro L., Strasser R.J. *et al*.: Effects of acute O_3 stress on PSII and PSI photochemistry of sensitive and resistant snap bean genotypes (*Phaseolus vulgaris* L.), probed by prompt chlorophyll "*a*" fluorescence and 820 nm modulated reflectance. – Plant Physiol. Bioch. **97**: 368-377, 2015.
Santos C.V.: Regulation of chlorophyll biosynthesis and degradation by salt stress in sunflower leaves. – Sci. Hortic.-Amsterdam **103**: 93-99, 2004.
Schansker G., Tóth S.Z., Strasser R.J.: Methylviologen and dibromothymoquinone treatments of pea leaves reveal the role of photosystem I in the Chl *a* fluorescence rise OJIP. – BBA-Bioenergetics **1706**: 250-261, 2005.
Sharkey T.D.: What gas exchange data can tell us about photosynthesis. – Plant Cell Environ. **39**: 1161-1163, 2016.
Sharkey T.D., Bernacchi C.J., Farquhar G.D. *et al*.: Fitting photosynthetic carbon dioxide response curves for C3 leaves. – Plant Cell Environ. **30**: 1035-1040, 2007.
Strasser R.J., Tsimilli-Michael M., Alaka S.: Analysis of the fluorescence transient. – In: Papageorgiou G.C., Govindjee (ed.): Chlorophyll *a* Fluorescence: a Signature of Photosynthesis. Pp. 321-362. Springer, Dordrecht 2004.
Strasser R.J., Tsimilli-Michael M., Qiang S. *et al*.: Simultaneous *in vivo* recording of prompt and delayed fluorescence and 820-nm reflection changes during drying and after rehydration of the resurrection plant *Haberlea rhodopensis*. – BBA-Bioenergetics **1797**: 1313-1326, 2010.
Thomas F.M., Gausling T.: Morphological and physiological responses of oak seedlings (*Quercus petraea* and *Q. robur*) to moderate drought. – Ann. Forest Sci. **57**: 325-333, 2000.
van Heerden P.D.R., Swanepoel J.W., Krüger G.H.J.: Modulation of photosynthesis by drought in two desert scrub species exhibiting C_3-mode CO_2 assimilation. – Environ. Exp. Bot. **61**: 124-136, 2007.
Wilson K.B., Baldocchi D.D., Hanson P.J.: Spatial and seasonal variability of photosynthetic parameters and their relationship to leaf nitrogen in a deciduous forest. – Tree Physiol. **20**: 565-578, 2000.
Yamori W., Evans J.R., von Caemmerer S.: Effects of growth and measurement light intensities on temperature dependence of CO_2 assimilation rate in tobacco leaves. – Plant Cell Environ. **33**: 332-343, 2010.
Yang C., Zhang Z.S., Gao H.Y., *et al*.: The mechanism by which NaCl treatment alleviates PSI photoinhibition under chilling-light treatment. – J. Photoch. Photobio. B **140**: 286-291, 2014.
Zhang L., Xing D.: Rapid determination of the damage to photosynthesis caused by salt and osmotic stresses using delayed fluorescence of chloroplasts. – Photochem. Photobio. Sci. **7**: 352-360, 2008.
Zivcak M., Brestic M., Balatova Z. *et al*.: Photosynthetic electron transport and specific photoprotective responses in wheat leaves under drought stress. – Photosynth. Res. **117**: 529-546, 2013.